# High resolution photographic imaging

**Felix Bettonvil**[1,2,3]

[1] **Sterrewacht Leiden, Universiteit Leiden, Niels Bohrweg 2, 2333 CA Leiden, The Netherlands**

[2] **NOVA Optical and Infrared Instrumentation Division at ASTRON, Oude Hoogeveensedijk 4, 7991 PD Dwingeloo, The Netherlands**

[3] **KNVWS Meteor Section, The Netherlands**

F.C.M.Bettonvil@strw.leidenuniv.nl

A high-resolution camera is described, based on DSLR technology and long focal length lens together with a 200 cycles/sec optical shutter, with the aim to collect higher accuracy orbital elements. The paper describes the design considerations, test setup, and analyses and discusses the first results.

## 1 Introduction

Trajectories in the atmosphere and an estimate of the velocity are required for the determination of meteor orbits. In optical imaging the velocity is traditionally measured with a rotating shutter (Millman, 1936; Kohoutek, 1959) in front of the lens or in between the lens and film or detector. The accuracy of this modulation, as well as the modulation speed and astrometric accuracy of the exposure determine how well the velocity of the meteor can be estimated.

In (Bettonvil, 2008) an alternative method for modulation was proposed, which does not rely on rotating choppers but instead on a Liquid Crystal (LC) optical shutter, which periodically switches between dark state and transparent, which was with success applied to an All-sky camera (Bettonvil, 2014). Recent developments of this technology have now made available even faster LCs, which allow for modulation frequencies up to 200 Hz and even more[1]. This opens the way to observations with higher resolution, which should enable determination of orbits with higher accuracy, allowing for more strict D-criteria (Galligan, 2001), as the parameter velocity is a sensitive parameter in the determination of the orbit. Obtaining orbits with higher accuracy is highly interesting as it allows detection of fine structures in meteoroid streams at a more detailed level.

This paper, i) describes the details of a high-resolution camera based on the LC shutter technology, ii) presents the first results obtained with this system and iii) discusses them.

## 2 Design

The basis of the system is one of the fast Liquid Crystal optical shutters, as manufactured by LC-Tec, Borlänge, Sweden[1]. From the various types they produce, the X-FOS(G2) type was chosen, having open/closing times of 50µs/1.6ms, and with ~130EUR/pcs at reasonable cost/performance ratio. The switching behavior allows for modulation frequencies up to several hundreds cycles/sec. The modulation signal is achieved through a standard crystal based function generator, typically specified at frequency accuracies at $10^{-6}$ and stabilities at $10^{-6}$ level, which is more than sufficient for our needs.

*Figure 1* – Setup of the high-resolution camera: Canon EOS 1100D with Nikkor 50mm F/2 lens and in between (not visible, LC-TEC X-FOS(G2) optical shutter. The function generator for shutter control is visible below the tripod (in blue), as well as an exposure controller.

[1] http://www.lc-tec.com/optical-shutter

An improved plate scale is achieved by increasing the focal length of the system. Here a wide range of lenses was analyzed and an optimum searched for orbit accuracy and sensitivity/yield. The parameter chosen to be optimized is the multiple of both, as both the aim is to increase accuracy, but on the same time not decreasing yield to negligible numbers, which in the extreme case would result in no statistical relevance. Finally, a 50mm F/2 was chosen as best for the first tests, giving a Field of View of 25 x 17 deg$^2$.

Similar as chosen in the design of the All-sky camera (Bettonvil, 2014), the shutter is built between camera and lens. For the test a Canon EOS, 1100D was used, equipped with a 12.2 MPxl sensor. *Figure 1* gives an overview of the entire camera setup.

## 3 Test setup and results

A first test was scheduled during the Perseids meteor shower, in August 2014 from Bosnia. Despite the non-perfect conditions (i.e. full moon), this major shower should anyhow result in a number of recordings.

In order to optimally capture the meteor trails, the camera was oriented such that the long axis of the detector was always reasonable well aligned with the radiant. This was done manually by realigning the camera around the third axis of the tripod periodically according to a pre-computed table. This ensured that the meteor in theory would travel over a maximum of pixels.

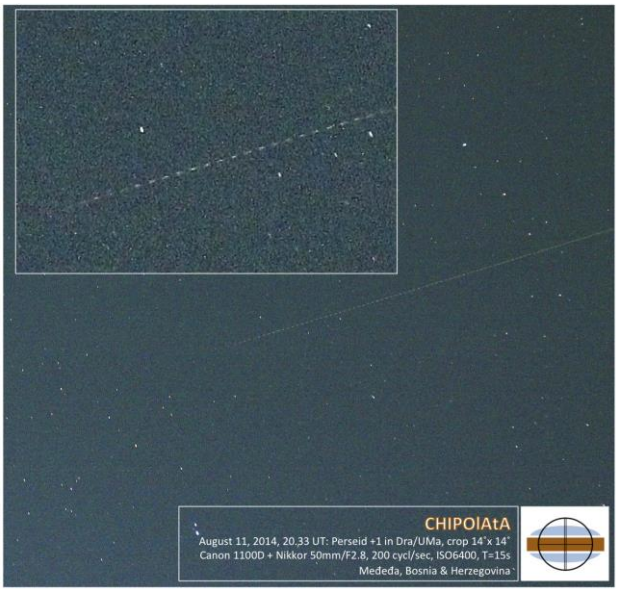


*Figure 2* – Example of Perseid as captured with the camera on August 11, 2014, 20.33 UT: Perseid +1 in Dra/UMa, crop 14° x 14°, Canon 1100D + Nikkor 50mm/F2.8, 200 cycl/sec, ISO6400, T=15s, Međeđa, Bosnia & Herzegovina. The entire trail contains 82 breaks.

For the first test, single station observations were performed, meaning that in theory no orbit could be determined. Nevertheless an estimate could be made based on assumptions on the typical height of (Perseid) meteors. In first order this should give sufficient insight in how well the velocity could be estimated and its impact on the orbital elements.

Camera sensitivity was chosen at ISO 6400 (max for EOS 1100D, diaphragm set to F/2.8 to enhance image quality, and exposure times 15s. Various modulation frequencies were tested (50-100-200 cycl/sec.).

During 9 nights, 13000 exposures were made, which delivered a modulated airplane and 10 meteor trails. The nicest example is reproduced in *Figure 2*.

## 4 Reduction

Aim of this first test was to analyze which accuracy can be achieved for the orbit. As for this test, as mentioned in the previous section, no double station was available, an assumption was made, as illustrated in *Figure 3*. First, astrometry was done of the real station 'A'. Then we assumed that from a fictive station 'B' the meteor was seen through both zenith and radiant, together forming a (vertical) plane. This plane and the plane through station 'A' and the meteor, then were intersected, with the exact location of station 'B' still a variable. The station location was moved around until the meteor appeared on a proper height (in our case the begin- and end height being 103 respectively 94km).

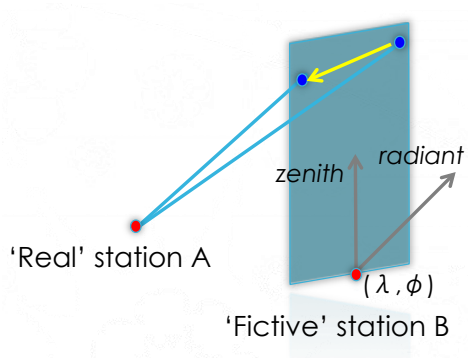


*Figure 3* – Principle of estimation of the atmospheric trajectory. For explanation see text.

In this paper we focus entirely on analysis of the meteor of *Figure 2*. The trail shows 82 breaks and spans ~1500 detector pixels, lasting for ~0.3sec. Evidently, only the last part of the trail is captured.

Astrometry of the image was done with help of the online astrometry tool astrometry.net[2]. Due to the only small optical distortion apparent in the image, this gave acceptable results for this test. The obtained plate relation between (x,y) pixel values and (R.A., declination) sky coordinates was double checked with SAO Image DS9.

A rough indication of the brightness of the meteor was done by comparing the break with maximum brightness with a star showing equal counts, and neglecting any spectral difference. Based on this approximation a meteor brightness of ~$M_v$ = +1 was found.

[2] http://astrometry.net/

For estimation of the velocity several measurement methods were tested:

1) manual measurement of the start of all breaks (blue curve in *Figure 3*)
2) Centroiding of all breaks (green curve in *Figure 3*)
3) Fast Fourier Transform of the entire trail.

For all methods, the pixel coordinates of all breaks were obtained from the image, transformed into (R.A., declination) coordinates and then into (h, Az) coordinates. Through all (h,Az) directions a plane is then constructed and intersected with the other plane from the fictive station. The intersection line represents the atmospheric trajectory. The 3D velocities are finally obtained by deriving the points of minimum distance between the direction vector of each break and the atmospheric intersection line.

Method 1 and 2 show that there is not much difference between them, with similar break-to-break variations. A fit through all data points also indicates that no clear evidence of deceleration can be found. With break #1 the beginning of the trail and break #82 the end, the small change in velocity even points the other way around. In the remainder of this paper I assume therefore no deceleration is present, and focus because of this on deriving the *average* velocity.

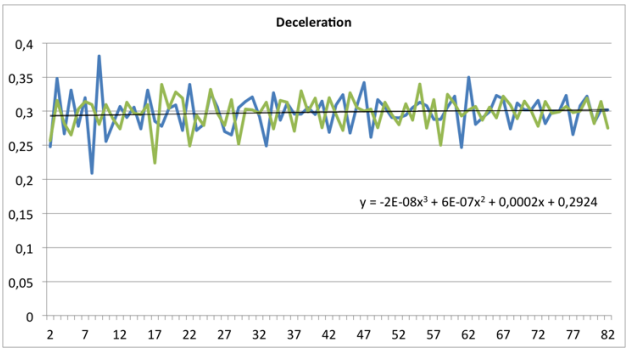


*Figure 4* – Measurement of centroids along trails (manual measurement – blue; centroiding – green). The black line represents a fit through all data.

In case of method 1 and 2, for deriving the average velocity, from all measurement points the typical velocity measurement error was estimated, being in the order of 5%. Then three successive points on both beginning and end of the trajectory were identified, of which all three have minimal deviation from the average velocity. These points are regarded as a good representation of the average velocity. The average velocity follows then from the total span of breaks between the two points, divided by the time span, and the accuracy from the average measurement accuracy of all 82 data points. *Table 1* gives the results. No other filtering is applied, e.g. RANSAC as described in (Egal, 2014).

The third method is based on transformation of the trajectory from time domain into frequency domain with the help of the Fast Fourier Transform as introduced in (Bettonvil, 2008). The dominant frequency represents the apparent velocity, which then is converted into a 3D velocity. The estimate for the accuracy is obtained from the deviation of the fit of a Gaussian through the frequency peak (Bettonvil, 2008).

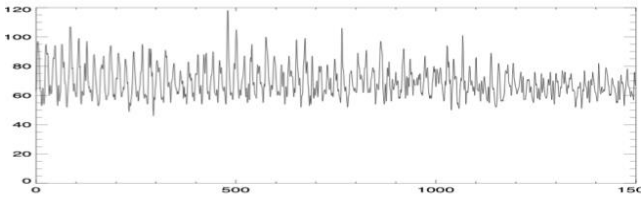

*Figure 5* – Intensity profile through the center of the entire meteor trail.

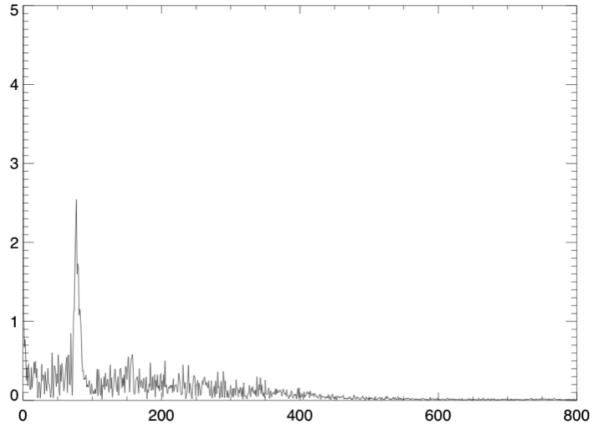

*Figure 6* – FFT of the intensity profile of *Figure 5*.

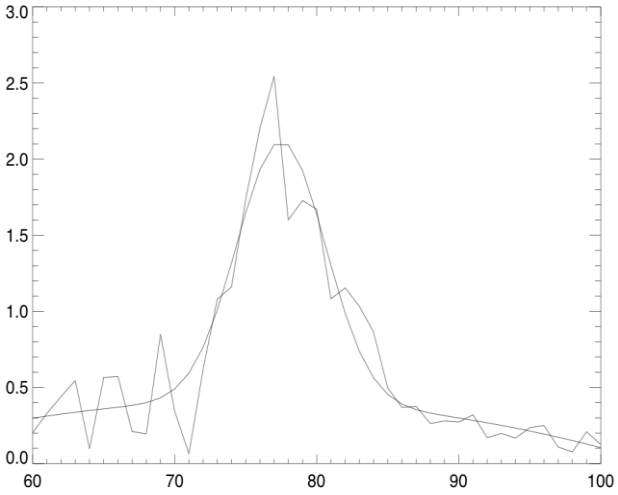

*Figure 7* – Detail of Figure 6, with Gaussion fit through the peak.

*Table 1* – Derived velocities for all applied methods.

| Method | Velocity |
|---|---|
| Spatial measurement (Method 1, 2) | 59,63 ± 0,04 km/s (± 0,06%) |
| FFT (Method 3) | 59,61 ± 0,04 km/s (± 0,06%) |

## 5 Discussion

All methods for the determination of the velocity are in good agreement with each other. In order to get insight in the effect of the velocity on the orbit, the heliocentric orbit elements and associated errors were calculated, solely based on the estimated error in the velocity. No other errors were taken into consideration. *Table 2* lists the results. The semi major axis for this (fictive) example is 23.3 +/- 2AU. *Figure 8* illustrates how the obtained accuracy fits within the entire sample of IAU orbits.

*Table 2* – Orbital elements for the Perseid meteor as analyzed.

| Orbit: | | | | |
|---|---|---|---|---|
| Astr. longitude of ascending node | (OMEGA) | [deg]: | 138.901 | +/- 0.000 |
| Inclination | (i) | [deg]: | 118.906 | +/- 0.023 |
| Argument of perihelion | (omega) | [deg]: | 158.985 | +/- 0.044 |
| Semi major axis | (a) | [AU]: | 23.2836 | +/- 2.0413 |
| Distance sun ~ perihelion | (q) | [AU]: | 0.9805 | +/- 0.0001 |
| Distance sun ~ aphelion | (Q) | [AU]: | 45.5868 | +/- 4.0824 |

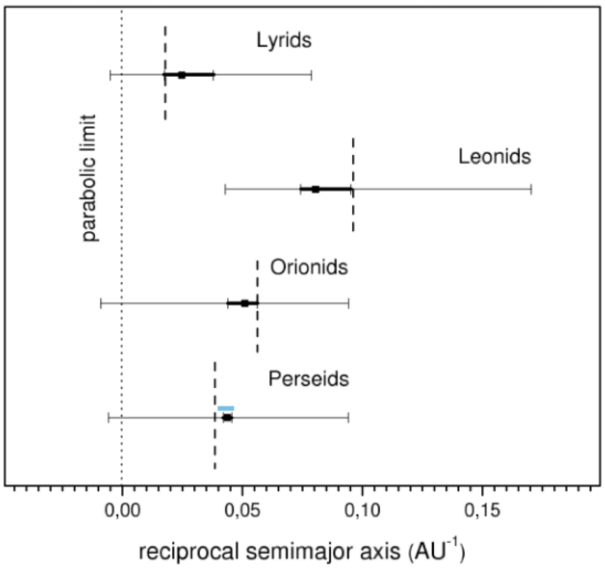


*Figure 8* – Reciprocal semi major axis, inserted in a plot from Hydukova of all orbits of th IAU database (from Hydukova Jr, 2011).

## 6 Conclusions

The first test with the high-resolution camera showed that indeed high accuracy can be obtained, with several analysis methods being in good agreement. No deceleration could be measured from the analyzed meteor.

After this successful initial test, the aim is now to obtain a larger data sample, involving more than one shower. These observations will be done on the basis of double station work, allowing for proper orbit calculations.

Based on these results, another optimization can be done, to verify if a higher accuracy can be achieved by narrowing the field of view even more.

From the technical point of view, to further improvements are planned: 1) observing in RAW format (initial tests were carried out on jpg format; 2) motorizing the third axis of the camera mount, maintaining a proper alignment of the shower meteors and the detection field accurately.

## References

Bettonvil F. C. M. (2014). "Remote and automatic small-scale observatories: experience with an all-sky fireball patrol camera". In, Ramsay S. K., McLean I. S., and Takami H., editors, *Proceedings SPIE*, Ground-based and Airborne Instrumentation for Astronomy V, **9147**, id. 91473U, 9 pages.

Bettonvil F. (2008). "Determination of the Velocity of Meteors Based on Sinodial Modulation and Frequency Analysis". *Earth, Moon, and Planets*, **102**, 205–208.

Egal A., Vaubaillon J., Colas F., Atreya P. (2014). "Low dispersion meteor velocity measurements with CABERNET", In Rault J.-L., and Roggemans P., editors, *Proceedings of the International Meteor Conference*, Giron, France, 18–21 September 2014. IMO, pages???–???.

Galligan D. P. (2001). "Performance of the D-criteria in recovery of meteoroid stream orbits in a radar data set". *Monthly Notices of the Royal Astronomical Society*, **327**, 623–628.

Hajdukova M. Jr. (2011). "The orbital dispersion in the long-period meteor streams". *Contrib. Astron. Obs. Skalnaté Pleso*, **41**, 15–22.

Kohoutek L. (1959). "On the precision of the photographic determination of the geocentric meteor velocity". *Bulletin of the Astronomical Institute of Czechoslovakia*, **10**, 120–132.

Millman P. M. (1936). "Meteor News - A Brilliant Fireball; Meteor Photographs taken with a Rotating Shutter; Effect of Observing Conditions on Meteor Rates". *Journal of the Royal Astronomical Society of Canada*, **30**, 101–104.